



SMARCA3, a Chromatin-Remodeling Factor, Is Required for p11-Dependent Antidepressant Action

Yong-Seok Oh,¹ Pu Gao,³ Ko-Woon Lee,¹ Ilaria Ceglia,¹ Ji-Seon Seo,¹ Xiaozhu Zhang,¹ Jung-Hyuck Ahn,⁴ Brian T. Chait,² Dinshaw J. Patel,³ Yong Kim,^{1,*} and Paul Greengard^{1,*}

¹Laboratory of Molecular and Cellular Neuroscience

²Laboratory of Mass Spectrometry and Gaseous Ion Chemistry

The Rockefeller University, New York, NY 10065, USA

³Structural Biology Program, Memorial Sloan-Kettering Cancer Center, New York, NY 10065, USA

⁴Department of Biochemistry, Ewha Womans University School of Medicine, Yangcheon-ku, Seoul 158-710, Republic of Korea

*Correspondence: kimyo@rockefeller.edu (Y.K.), greengard@rockefeller.edu (P.G.)

<http://dx.doi.org/10.1016/j.cell.2013.01.014>

SUMMARY

p11, through unknown mechanisms, is required for behavioral and cellular responses to selective serotonin reuptake inhibitors (SSRIs). We show that SMARCA3, a chromatin-remodeling factor, is a target for the p11/annexin A2 heterotetrameric complex. Determination of the crystal structure indicates that SMARCA3 peptide binds to a hydrophobic pocket in the heterotetramer. Formation of this complex increases the DNA-binding affinity of SMARCA3 and its localization to the nuclear matrix fraction. In the dentate gyrus, both p11 and SMARCA3 are highly enriched in hilar mossy cells and basket cells. The SSRI fluoxetine induces expression of p11 in both cell types and increases the amount of the ternary complex of p11/annexin A2/SMARCA3. SSRI-induced neurogenesis and behavioral responses are abolished by constitutive knockout of SMARCA3. Our studies indicate a central role for a chromatin-remodeling factor in the SSRI/p11 signaling pathway and suggest an approach to the development of improved antidepressant therapies.

INTRODUCTION

Selective serotonin reuptake inhibitors (SSRIs) are currently the most widely used class of antidepressants (Berton and Nestler, 2006). SSRI medications generally take several weeks to show clinical efficacy, including mood elevation, despite their immediate effect on serotonergic neurotransmission. This therapeutic delay suggests the involvement of complicated downstream mechanisms, including long-term changes in gene expression and neuroplasticity. However, our knowledge of the molecular mechanisms underlying the efficacy of long-term treatment with SSRIs and of the pathophysiology of depression is still rudimentary.

p11 (S100A10) is a pivotal regulator of depression-like behaviors and a mediator of antidepressant responses (Svenningsson et al., 2006). Despite the importance of p11 in the actions of SSRIs, our knowledge about its underlying molecular mechanisms is limited (Svenningsson et al., 2006). Annexin A2 (AnxA2) is a well-characterized binding partner for p11. AnxA2, together with p11, plays a role in trafficking of membranous/cytoplasmic proteins to plasma membrane or in providing them with firm anchorage at the plasma membrane and the cytoskeletal structure (Rescher and Gerke, 2008). p11 and AnxA2 were also found to localize in the nucleus and interact with nuclear proteins (Das et al., 2010; Liu and Vishwanatha, 2007), although the precise roles of p11 and AnxA2 in the nucleus have not been clearly defined. In this study, we have observed that chronic treatment with an SSRI, fluoxetine (FLX), increases the levels of the p11/AnxA2 complex. We have identified SMARCA3, a chromatin-remodeling factor, as a downstream target of the p11/AnxA2 complex. Our data indicate that the p11/AnxA2/SMARCA3 pathway mediates both neurogenic and behavioral responses to SSRIs.

RESULTS

Identification of SMARCA3 as a Specific Binding Partner of p11/AnxA2 Complex

p11, together with AnxA2, forms a heterotetramer in cells. However, it is not yet established that p11 exists in a protein complex with AnxA2 in brain tissue. Here, we show that the protein level of AnxA2 is drastically downregulated in the frontal cortex and hippocampus of p11 knockout (KO) mice (Figure 1A), despite unchanged levels of AnxA2 transcript (Figure 1B). In contrast, the protein level of AnxA1, another annexin family member, and of S100B, another S100 family member, was not altered in the brain of p11 KO mice, indicating the specificity of the physiological interaction between p11 and AnxA2 in the brain (Figure 1A). We have also observed that p11 protein level in the hippocampal lysates from AnxA2 KO mice is reduced (data not shown). Given that components of a protein complex often stabilize each other, the data strongly support the existence of

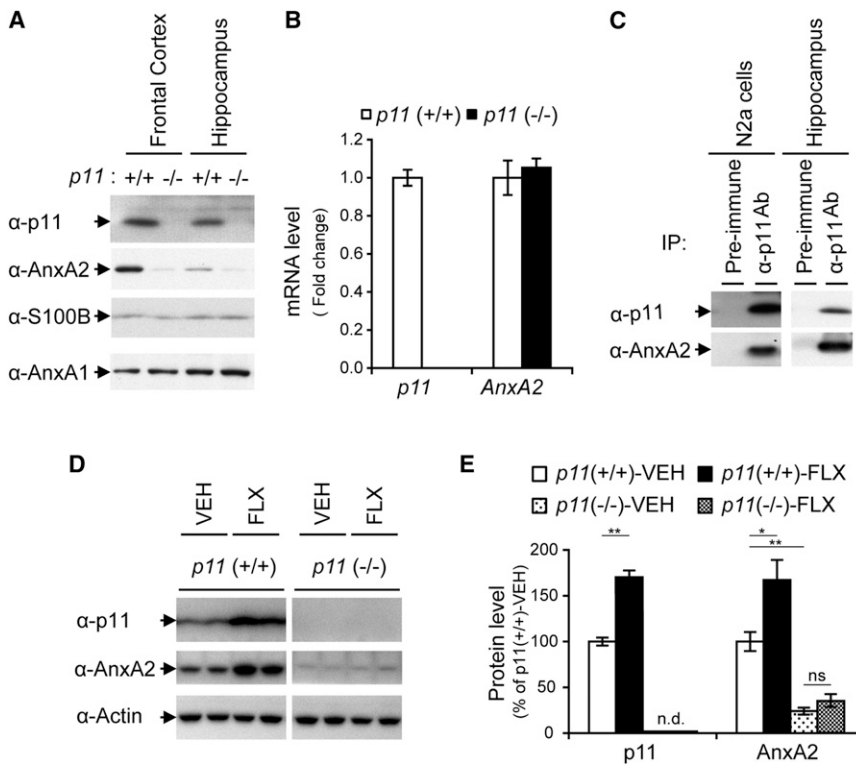


Figure 1. p11/AnxA2 as an Antidepressant-Regulated Protein Complex

(A) Brain lysates from frontal cortex and hippocampus of WT (+/+) and *p11* KO (-/-) mice were immunoblotted for p11, AnxA2, S100B, and AnxA1.

(B) mRNA levels of *p11* and *AnxA2* in the hippocampus were measured using qPCR in WT (+/+) and *p11* KO (-/-) mice. Data represent mean \pm SEM.

(C) Coimmunoprecipitation of p11 and AnxA2 from lysates of N2a neuroblastoma cells and mouse hippocampus using anti-p11 antibody. IP, immunoprecipitate.

(D) WT (+/+) or *p11* KO (-/-) mice were administered VEH or FLX for 2 weeks. Hippocampal lysates were immunoblotted for p11, AnxA2, and β -actin.

(E) Quantitation of the immunoblot shown in (D) using infrared imaging system (Odyssey; LI-COR). Data represent mean \pm SEM. * $p < 0.05$ and ** $p < 0.01$, t test. ns, nonsignificant; n.d., not detectable.

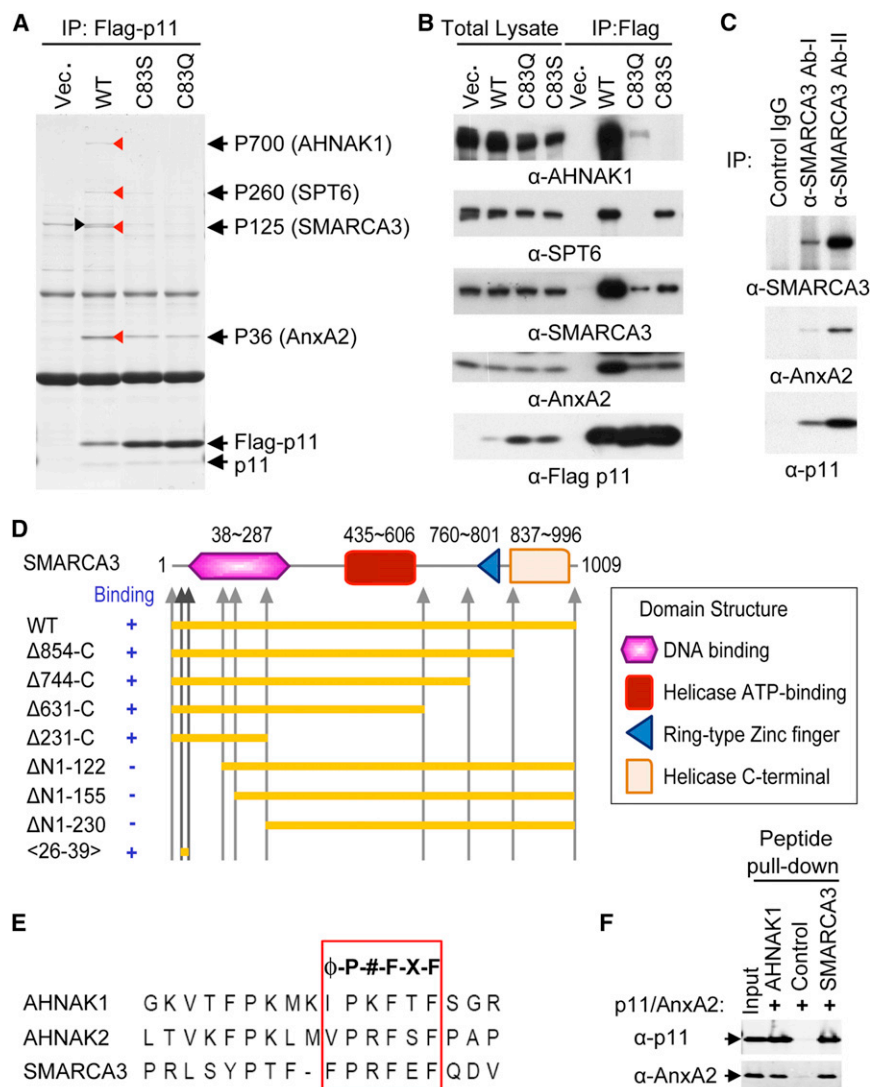
a protein complex of p11 and AnxA2 in the brain. In addition, we were able to coimmunoprecipitate AnxA2 with p11 from lysates of the hippocampus as well as from lysates of N2a neuroblastoma cells (Figure 1C).

Previous studies showed that p11 was induced in the frontal cortex (Svenningsson et al., 2006) and hippocampus (Warner-Schmidt et al., 2010) by chronic administration of antidepressants. In the present study, we observed concomitant upregulation of p11 ($170.4\% \pm 7.3\%$ of *p11*(+/+)-vehicle (VEH) group; $p = 0.004$) and of AnxA2 ($167.1\% \pm 20.8\%$; $p = 0.042$) (Figures 1D and 1E). This AnxA2 increase was not observed in *p11* KO mice (Figure 1E). Collectively, these results suggest that p11 and AnxA2 exist as a protein complex, which can be induced by antidepressant administration.

Next, we undertook a search for binding partners for p11/AnxA2. To ensure the specificity of the interaction with the p11/AnxA2 heterotetramer, we compared wild-type (WT) versus C83S and C83Q mutants of p11, which prevent the interaction between p11 and AnxA2 (Kube et al., 1992). C83S and C83Q mutations in p11 significantly decreased the interaction with AnxA2, without altering the interaction with endogenous p11 to form a p11 dimer, suggesting that C83 mutations selectively interfere with the heterotetramer formation, but not the homodimerization of p11 molecules (Figure S1A available online). After transfection of *p11* WT and C83 mutant plasmids into HEK293 cells, we isolated the protein complex of p11 using immunoprecipitation (Figure 2A). Four proteins with relative molecular mass of 700, 260, 125, and 36 kDa were coprecipitated with WT p11 and were identified by mass spectrometry as AHNAK1 (AHNAK nucleoprotein), SPT6 (suppressor of Ty 6 homolog *S. cerevisiae*),

SMARCA3 (SWI/SNF-related, matrix-associated, actin-dependent regulator of chromatin, subfamily A, member 3), and AnxA2, respectively (Figure 2A). The identity of each protein was further confirmed by immunoblotting with specific antibodies (Figure 2B). AHNAK1, SPT6, and SMARCA3 were coprecipitated with WT p11, and the interaction was greatly reduced or abolished by either C83S or C83Q mutation of p11, indicating that the interaction likely needs AnxA2 binding to p11. AHNAK1 has been reported as a binding protein of p11/AnxA2 (Benaud et al., 2004). We focused on SMARCA3 in the following studies because of the potential physiological importance of this chromatin-remodeling factor. To evaluate the role of AnxA2 in the intermolecular interaction, an in vitro pull-down assay using GST-p11, AnxA2, and 35 S-labeled SMARCA3 was used. The SMARCA3 interaction was significantly increased by the addition of AnxA2 to the pull-down assay mixture (Figure S1B). The interaction of SMARCA3 with p11/AnxA2 was further confirmed by the inverse immunoprecipitation using anti-SMARCA3 antibodies (Figure 2C). Collectively, these results identified SMARCA3 as a binding partner of p11/AnxA2.

SMARCA3 belongs to the family of SWI/SNF proteins that use the energy of ATP hydrolysis to remodel chromatin in a variety of nuclear processes, such as transcriptional regulation, and DNA replication and repair (Debaue et al., 2008). SMARCA3 contains multiple domain structures, including DNA-binding, helicase ATP-binding, RING-type Zinc finger, and helicase C-terminal domains (Figure 2D). We next performed in vitro pull-down assay with a series of deletion constructs of SMARCA3 to determine the binding region for p11/AnxA2 (Figures 2D, S1C, and S1D). Although the serial deletion from the SMARCA3 C terminus had no effect on the interaction with p11 (Figure S1C), the deletion of the N terminus of SMARCA3 abolished the interaction (Figure S1D), localizing a binding region close to the N terminus of SMARCA3 (Figure 2D). Through sequence alignment between



AHNAK family proteins and the N terminus of SMARCA3, we found a highly conserved putative binding motif, represented by Φ -P-#-F-X-F (Φ , hydrophobic amino acid; P, proline; #, basic amino acid; F, phenylalanine; X, any amino acid) (Figure 2E). Next, we performed a peptide pull-down assay to validate p11/AnxA2 binding to the putative binding motif. Indeed, the short synthetic peptides from AHNAK1, AHNAK2, and SMARCA3 covering the putative motif were sufficient to bind to p11/AnxA2 (Figure 2F; data not shown for AHNAK2 peptide).

Crystal Structure of p11/AnxA2 Bound to Its Ternary Target, SMARCA3

To understand the molecular interaction of SMARCA3 and AHNAK1 with p11/AnxA2 in detail, we conducted structural studies of p11 and AnxA2 complexed with SMARCA3 or AHNAK1 peptides. We have used a p11-AnxA2 fusion protein (henceforth named p11-AnxA2 peptide cassette) in which p11 (1-92) is connected to AnxA2 peptide with a nine amino

Figure 2. Identification of the Binding Proteins of p11/AnxA2 Complex

(A) Control vector (Vec.) and vectors containing WT or interaction-defective mutants (C83S and C83Q) of p11 were transfected into HEK293 cells. Proteins that coprecipitated with WT are marked with arrowheads (red). A nonspecific band is indicated by a black arrowhead. The proteins were identified by tandem mass spectrometry (black arrows). (B) Immunoblots for AHNAK1, SPT6, SMARCA3, AnxA2, and Flag-p11, as indicated. (C) Coimmunoprecipitation of p11/AnxA2/SMARCA3 complex from brain lysates by two different anti-SMARCA3 antibodies. (D) WT, deletion mutants, and a peptide were tested for their interaction with p11/AnxA2. (E) Putative p11-binding sequences of AHNAK1 (aa 5654–5671), AHNAK2 (aa 5382–5399), and SMARCA3 (aa 26–42). (F) Interaction of the AHNAK1 or SMARCA3 peptides with p11/AnxA2 was confirmed by the pull-down assay of biotinylated peptides. Scrambled peptide was used as control. See also Figure S1.

acid linker (QENLYFQGD) (Rezvanpour et al., 2009) to generate complexes with added SMARCA3 (P26-F39) and AHNAK1 (G5654-F5668) peptides. Crystals of the complexes with SMARCA3 peptide (Figure 3) and AHNAK1 peptide (Figure S2) diffracted to 3.0 and 2.0 Å resolution, respectively. The structures of the two complexes exhibited similar recognition principles; although the peptide sequences are different, the backbones of bound SMARCA3 and AHNAK1 peptides superimpose well with an rmsd of 0.4 Å. The higher-resolution structure of the AHNAK1 peptide complex (Figures

S2A–S2F) proved useful in resolving ambiguities in the lower-resolution structure of the SMARCA3 peptide complex (Figures 3A–3F).

We have solved the 3.0 Å crystal structure of the complex between SMARCA3 (P26-F39) peptide and the p11-AnxA2 peptide cassette (Figures 3A and 3B; crystallization statistics in Table S1). The fusion linker does not affect the binding between p11 and AnxA2 peptide because we observe the same intermolecular contacts in this complex as those reported previously for nonlinked components (Réty et al., 1999). The p11-AnxA2 peptide cassette forms a symmetrical dimer, with individual SMARCA3 peptides (electron density for bound peptide shown in Figure 3C), binding each monomer in the dimer, while retaining 2-fold symmetry (Figures 3A and 3B). Complex formation between SMARCA3 and p11-AnxA2 peptide cassette is mediated by van der Waals contacts and hydrogen bond interactions, whereby the SMARCA3 peptide interacts with elements of both p11 and AnxA2 peptide (Figure 3D). Two highly conserved amino

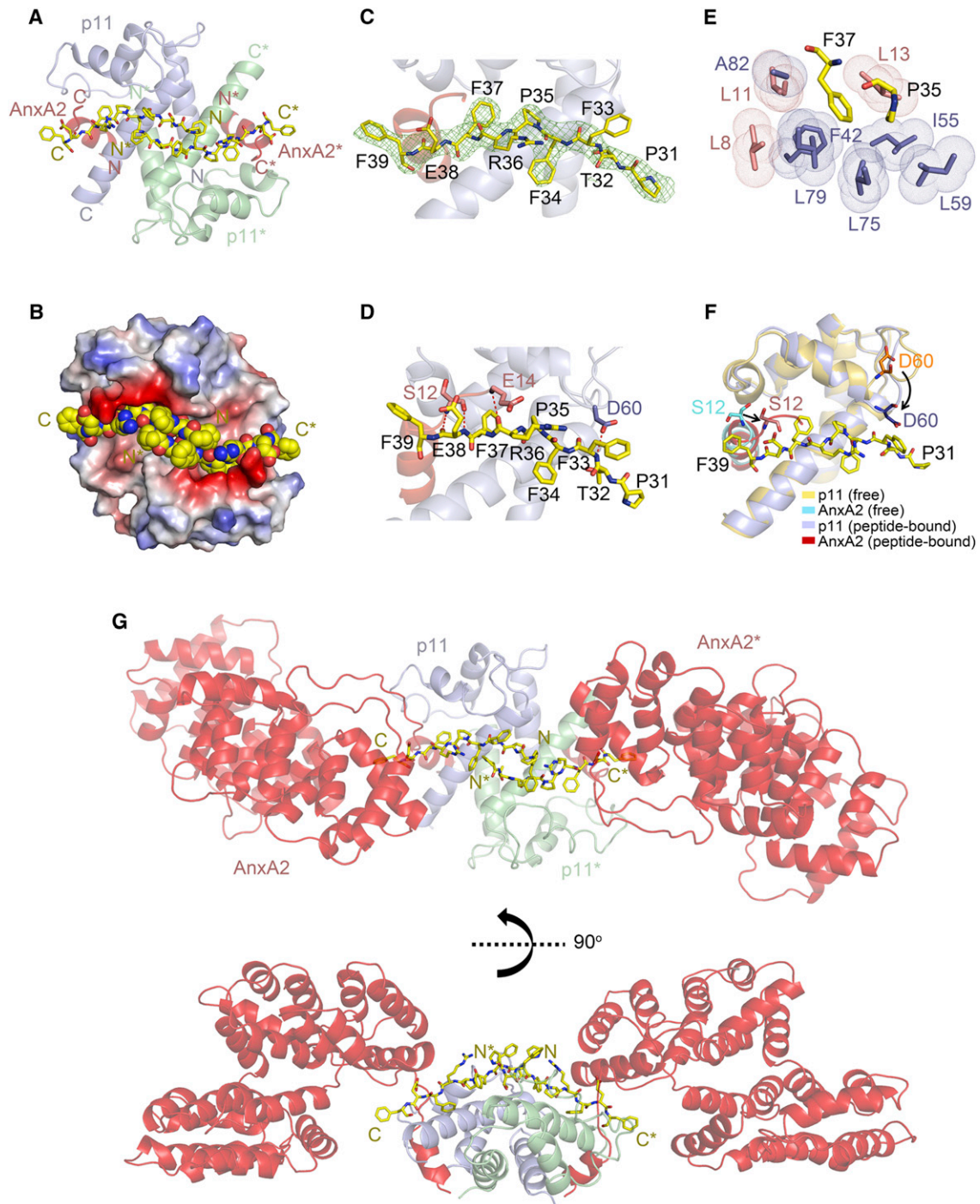


Figure 3. Crystal Structure of SMARCA3 Peptide Bound to p11-AnxA2 Peptide Cassette as Binary Complex and to p11 and Full-Length AnxA2 as Ternary Complex

(A) Ribbon view of crystal structure of p11-AnxA2 peptide cassette in complex with SMARCA3 peptide. p11 (blue and green) and AnxA2 peptide (salmon) are shown in ribbon, with the bound SMARCA3 peptides (yellow) in stick representations.

(B) Space-filling (peptide) and electrostatic surface (p11-AnxA2 peptide cassette) view of the complex illustrating the positioning of the pair of SMARCA3 peptides within the binding groove of the dimeric complex.

(C) Omit $2F_o - F_c$ electron density maps contoured at 1σ level of bound SMARCA3 peptide in one monomer of the complex. AnxA2 peptide (salmon) and p11 (blue) are represented in ribbon views, SMARCA3 peptide (yellow) is represented in a stick view, and electron density contours are in green.

(D) Intermolecular contacts within one monomer of the complex between the SMARCA3 peptide (yellow) and p11 (blue)-AnxA2 peptide (salmon) cassette, with hydrogen bonds depicted as red dashed lines.

(legend continued on next page)

acids (Pro35 and Phe37) in the bound SMARCA3 peptide are directed inward and anchored within a hydrophobic pocket formed by residues from both p11 (Phe42, Ile55, Leu59, Leu75, Leu79, and Ala82) and AnxA2 peptide (Leu8, Leu11, and Leu13) in the complex (Figure 3E), with similar interactions observed for Pro5664 and Phe5666 in the AHNAK1 complex (Figure S2E). The complex is stabilized by additional intermolecular hydrogen bonding interactions involving Phe33(SMARCA3)-Asp60(p11) and Arg36/Glu38(SMARCA3)-Ser12/Glu14(AnxA2 peptide) pairs (Figure 3D), with similar intermolecular contacts observed in the AHNAK1 complex (Figure S2D). In addition, the two bound SMARCA3 peptides are aligned in a head-to-head arrangement that is stabilized through intermolecular hydrogen bond formation between their N-terminal residues (Figure 3A). As expected, two point mutations (Pro35A and Phe37Y) in the binding consensus motif of SMARCA3 diminished the interaction with p11/AnxA2 (Figure S3A). In addition, Leu13A mutation of AnxA2 abolished the interaction with SMARCA3 with no effect on p11 interaction, whereas Leu8A and Leu11A mutation blunted the interaction to p11 as well as to SMARCA3 (Figure S3B), showing a unique role of the Leu13 residue in creating a binding pocket for the ternary targets. These structural and mutagenesis studies account for the molecular basis of the preferential binding of SMARCA3 to p11/AnxA2.

We compared the structures of p11-AnxA2 peptide cassette in the free (Protein Data Bank [PDB] ID code 1BT6) and SMARCA3 peptide-bound states following structural superimposition (Figure 3F). We observe that Asp60 in p11 is looped out from the peptide-binding groove in the free state but flips inward by 4.8 Å on complex formation with the bound SMARCA3 peptide, in the process forming additional intermolecular hydrogen bonds (Figure 3D). In addition to this change, the Asp58-Asp64 loop segment also undergoes a conformational change by shifting toward and completes the peptide-binding groove on complex formation (Figure 3F). A similar conformational transition is observed on addition of AHNAK1 peptide to the p11-AnxA2 peptide cassette (Figure S2F). Indeed, the mutation on the p11 Asp60 residue abolished the interaction with SMARCA3 while maintaining homodimerization of p11, as well as heterotetramer formation with AnxA2, although the D60A mutant of p11 displayed a decrease in protein stability (Figure S3C). In our structures of complexes with bound SMARCA3 and AHNAK1 peptides, the disulfide bridges observed for both p11 alone and the p11-AnxA2 peptide cassette (Réty et al., 1999) are disrupted due to the movement of the Asp58-Asp64 loop on complex formation. As to the conformational change in AnxA2, we observe an inward flip of Ser12 toward the peptide-binding site by 4.6 Å for the SMARCA3-bound complex, thereby forming intermolecular hydrogen bonds with bound peptide in the complex (Figures 3D and 3F). In addition, due to this movement

of Ser12, adjacent Leu13 in AnxA2 contributes to the closing of an additional face of the hydrophobic pocket, thereby anchoring the conserved residues Pro35 and Phe37 of bound SMARCA3 within the binding channel.

We have also successfully grown 2.8 Å crystals of SMARCA3 peptide bound to p11 and full-length AnxA2, with two views of the structure of the ternary complex shown in Figure 3G (X-ray statistics summarized in Table S2). Importantly, the crystal structure of p11/full-length AnxA2/SMARCA3 peptide illuminated the three-dimensional organization of each component within the ternary complex (Figure 3G). Full-length AnxA2 is composed of an N-terminal p11-binding region and a C-terminal annexin repeat region with opposing convex and concave sides (Gerke et al., 2005). The convex side of AnxA2 faces the cellular membrane to mediate PIP₂ binding, and the concave side faces away from the membrane. Although two N-terminal peptides of AnxA2 contact the lateral/bottom side of the inverted p11 homodimer, two N-terminal peptides of SMARCA3 are anchored on the top position of the inverted p11 dimer while crossing each other. On the other hand, C-terminal annexin repeat regions of full-length AnxA2 are not involved in intermolecular recognition in the ternary complex. Furthermore, the C-terminal ends of the SMARCA3 peptides point downward, suggesting that the rest of the C-terminal parts of SMARCA3 including DNA-binding, ATP-dependent helicase, and Zinc finger domains are likely positioned opposite to the convex side of the annexin repeat region of AnxA2. This mode of ternary complex assembly may leave C-terminal annexin repeat regions of AnxA2 free to execute the binding to PIP₂ and actin without steric hindrance. Taken together, our structural data on the complex with full-length AnxA2 implicate additional regulatory mechanisms through extended molecular interactions via C-terminal annexin repeat region.

Regulation of SMARCA3 Activity through Direct Interaction with p11/AnxA2

SMARCA3 was initially cloned as a regulatory factor that binds to the target DNA motifs of several gene promoters and enhancers and was shown to regulate the transcription of tissue-specific target genes such as *PAI-1*, *β-globin*, and *prolactin* (Debauve et al., 2008). It is noteworthy that the p11-binding region (aa 34–39) of SMARCA3 is located adjacent to the DNA-binding domain (aa 38–287) and seems to be partially overlapped. This observation prompted us to examine whether p11/AnxA2 interaction may regulate the DNA-binding affinity of SMARCA3. SMARCA3 was known to interact with the *B box* element in the promoter of the *PAI-1* gene (Ding et al., 1996). We carried out an in vitro reconstitution assay using purified recombinant proteins and the *B box* oligonucleotide immobilized on beads. The oligonucleotide pull-down assay showed that SMARCA3 can

(E) Positioning of the conserved residues Pro35 and Phe37 of the bound SMARCA3 peptide within a hydrophobic pocket formed by residues from AnxA2 peptide (salmon) and p11 (blue).

(F) A view of the superimposed structures of the p11-AnxA2 peptide cassette in the free (p11 in yellow and AnxA2 peptide in cyan) and SMARCA3-bound (p11 in blue and AnxA2 peptide in salmon) states. Black arrows highlight the conformational changes in p11 and AnxA2 peptide upon complex formation.

(G) Two views of 2.8 Å structure of SMARCA3 peptide (yellow) in stick representation bound to full-length AnxA2 (salmon) and p11 (blue and green) in ribbon representation shown for two different angles.

See also Figures S2 and S3, and Tables S1 and S2.

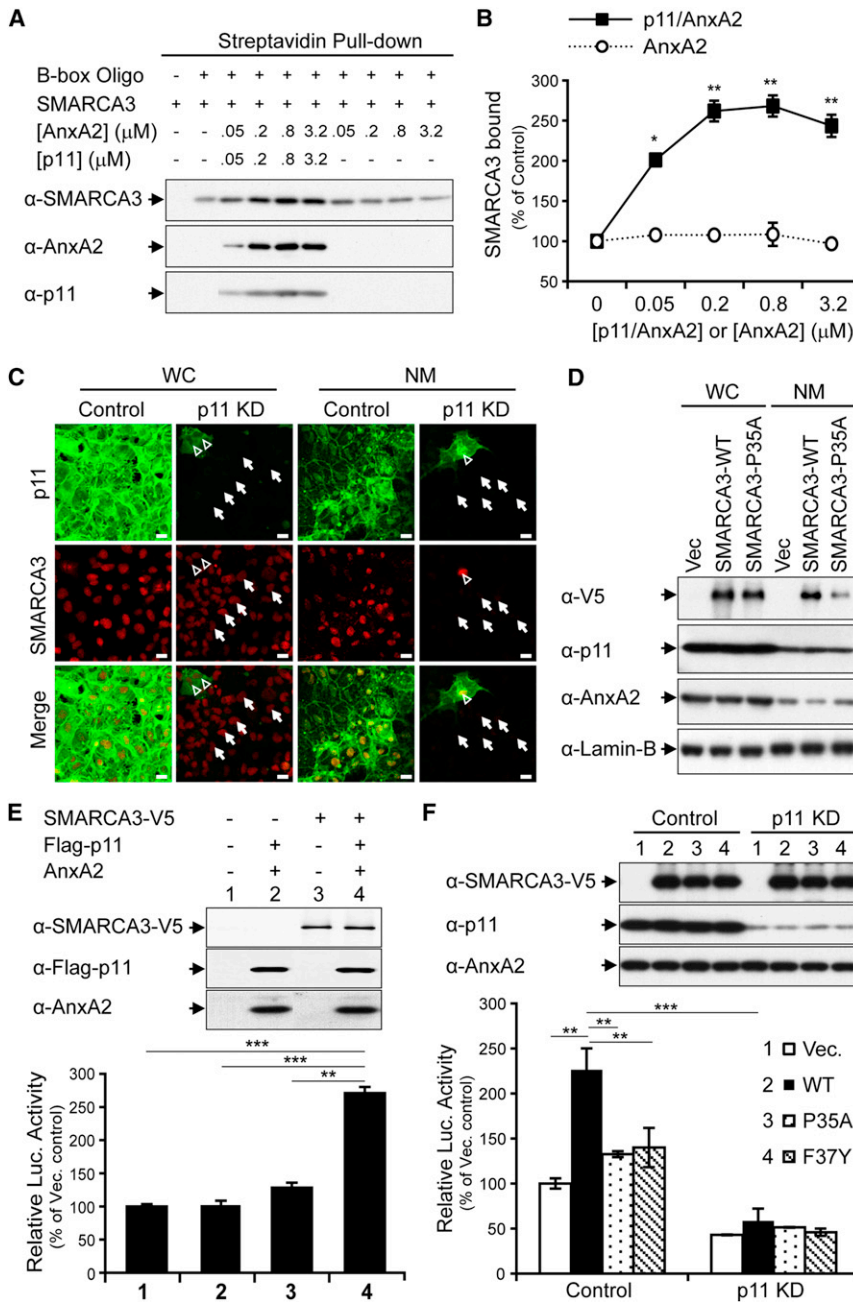


Figure 4. SMARCA3 Regulation by p11/AnxA2 Complex

(A) The *B* box oligonucleotide was incubated with the N-terminal domain of SMARCA3 (aa 1–350) and p11 and/or AnxA2. Bound proteins were immunoblotted.

(B) Quantitation of SMARCA3 bound to the *B* box oligonucleotide.

(C) Whole cells (WC) and the nuclear matrix (NM) were prepared from control (Control) or *p11*-knockdown (KD) COS-7 cells and immunostained with the indicated antibodies. Arrows indicate knockdown cells, and open arrowheads show nonknockdown cells. Scale bars, 20 μ m.

(D) Whole-cell lysates and NM were prepared from COS-7 cells transfected as indicated and immunoblotted for SMARCA3-V5 (α -V5), p11, AnxA2, and Lamin-B (nuclear matrix marker).

(E) Transcriptional activity of SMARCA3 in N2a cells after cotransfection of luciferase reporter gene conjugated to *PAI-1* promoter, together with indicated plasmids. Immunoblots of cell lysates and luciferase activity are shown.

(F) Transcriptional activity of SMARCA3 in Control or *p11*-knockdown (KD) COS-7 cells transfected with indicated SMARCA3 plasmids.

Mean \pm SEM. * p < 0.05, ** p < 0.01, and *** p < 0.001, t test.

form a quaternary complex together with p11/AnxA2 and the *B* box oligonucleotide (Figure 4A). Furthermore, p11/AnxA2 interaction increases the DNA-binding affinity of SMARCA3 by up to 2.5-fold, whereas the equivalent amount of AnxA2 alone did not show any effect (Figure 4B).

The distinct subnuclear localizations of nuclear factors are essential to conduct chromatin remodeling, transcription, replication, and mRNA processing (Zaidi et al., 2007). In fact, among SWI/SNF family chromatin remodelers, the hBAF (Brg1-associated factors) complex is known to be targeted to the nuclear matrix/chromatin through direct interaction with nuclear PIP₂

and actin/actin-related protein (Rando et al., 2002; Zhao et al., 1998). It is well established that p11/AnxA2 binds to PIP₂ as well as actin (Rescher and Gerke, 2008). Thus, we examined the possibility that p11/AnxA2 may regulate the subnuclear localization of SMARCA3. In the whole-cell preparation, p11 is predominantly cytoplasmic, and a much less but significant level of p11 is in the nucleus, whereas SMARCA3 is mainly localized inside the nucleus. Our unpublished studies with primary cultured neurons indicate that p11, together with AnxA2, shuttles between cytoplasm and nucleus (data not shown). In the nuclear matrix, which is prepared after cell permeabilization followed by chromatin digestion, the presence and the colocalization of p11 and SMARCA3 are evident (Figure 4C). Importantly, the retention of SMARCA3 in the nuclear matrix is dramatically reduced by the silencing of p11 expression with siRNA. Consistent with that, biochemical fractionation of the nuclear matrix revealed that WT SMARCA3 is in the nuclear matrix preparation, whereas the P35A mutant, defective in p11/AnxA2 interaction, is not (Figure 4D), confirming the importance of the p11/AnxA2 complex in the subnuclear localization of SMARCA3. Taken together, p11/AnxA2 not only increases the DNA-binding affinity of SMARCA3 but also anchors SMARCA3 to the nuclear matrix presumably via the interaction of AnxA2 with actin and PIP₂.

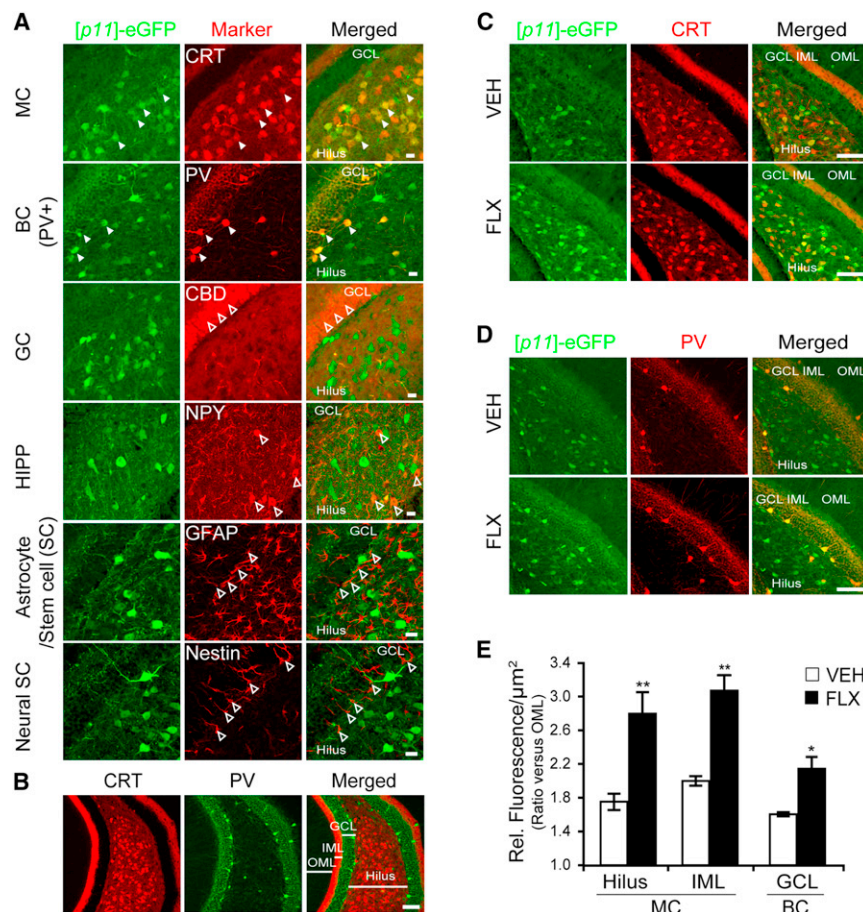


Figure 5. SSRI Regulates p11 Expression in Mossy Cells and Basket Cells in the Dentate Gyrus

(A) Cell types expressing [p11]-EGFP in the dentate gyrus. CRT (hilar mossy cells [MC]), parvalbumin (PV, subpopulation of basket cells [BC(PV+)]), calbindin (CBD, mature granule cells [GC]) neuropeptide Y (NPY, hilar interneurons perforant path [HIPP]), glial fibrillary acidic protein (GFAP, astrocytes), and nestin (neural stem cells [SC]) were used to identify cell types. Solid arrowheads indicate representative doubly labeled cells. Open arrowheads show cells labeled only with markers. Scale bars, 20 μ m.

(B) Distinct laminar projections of mossy cells and parvalbumin-positive basket cells in the dentate gyrus. GCL, granule cell layer; OML, outer molecular layer. Scale bar, 100 μ m.

(C–E) Induction of [p11]-EGFP in dentate gyrus by chronic SSRI. The dentate gyrus slices were costained with anti-EGFP antibody (C and D) and either anti-CRT (C) or anti-PV (D) antibodies. Scale bars, 100 μ m. EGFP intensity was quantitated in the indicated subregions (E). Values were normalized to fluorescence intensity in OML. Data represent mean \pm SEM (n = 5–6 mice per group). *p < 0.05 and **p < 0.01, t test. Rel. Fluorescence, relative fluorescence. See also Figure S4.

to show therapeutic effects. SMARCA3-mediated regulation of transcription may be associated with the therapeutic delay. Our previous study showed that p11 is expressed in GABAergic basket cells in

the dentate gyrus and might play a critical role in antidepressant-induced hippocampal neurogenesis (Egeland et al., 2010). We thus examined the neuronal types expressing p11 and SMARCA3 in the dentate gyrus. We took advantage of BAC (bacterial artificial chromosome) transgenic mice (Heintz, 2001), in which the expression of EGFP reporter is driven by p11 promoter activity ([p11]-EGFP). The excellence of immunostaining analysis using anti-EGFP antibody enabled us to visualize the entire neuronal processes of the neurons expressing p11. Because EGFP-positive neurons in the BAC-[p11]-EGFP mice are doubly positive for the immunostaining of endogenous p11, EGFP-positive neurons represent p11-expressing neurons (Figure S4A). p11-expressing cells assessed with [p11]-EGFP signal localize in the hilus region of the dentate gyrus (Figure 5A). To identify neuronal types for the p11-expressing neurons, hippocampal sections from BAC-[p11]-EGFP transgenic mice were doubly stained with EGFP and neuronal-type markers. Notably, [p11]-EGFP reporter signal was found to be enriched both in calretinin (CRT)-positive mossy cells and in PV-positive basket cells, whereas the signal was negligible in granule cells and is rarely (<5%) observed in HIPP cells (Figure 5A). Furthermore, p11 expression is not observed in astrocytes or neural stem cells (Figure 5A).

Regulation of the p11/AnxA2/SMARCA3 Complex in Hilar Mossy Cells and Basket Cells in the Dentate Gyrus

p11 mediates the actions of antidepressants (Svenningsson et al., 2006). Chronic antidepressant administration increased the level of p11 in the hippocampus (Figures 1D and 1E). Antidepressant actions including neurogenesis require several weeks

the dentate gyrus and might play a critical role in antidepressant-induced hippocampal neurogenesis (Egeland et al., 2010). We thus examined the neuronal types expressing p11 and SMARCA3 in the dentate gyrus.

We took advantage of BAC (bacterial artificial chromosome) transgenic mice (Heintz, 2001), in which the expression of EGFP reporter is driven by p11 promoter activity ([p11]-EGFP). The excellence of immunostaining analysis using anti-EGFP antibody enabled us to visualize the entire neuronal processes of the neurons expressing p11. Because EGFP-positive neurons in the BAC-[p11]-EGFP mice are doubly positive for the immunostaining of endogenous p11, EGFP-positive neurons represent p11-expressing neurons (Figure S4A). p11-expressing cells assessed with [p11]-EGFP signal localize in the hilus region of the dentate gyrus (Figure 5A). To identify neuronal types for the p11-expressing neurons, hippocampal sections from BAC-[p11]-EGFP transgenic mice were doubly stained with EGFP and neuronal-type markers. Notably, [p11]-EGFP reporter signal was found to be enriched both in calretinin (CRT)-positive mossy cells and in PV-positive basket cells, whereas the signal was negligible in granule cells and is rarely (<5%) observed in HIPP cells (Figure 5A). Furthermore, p11 expression is not observed in astrocytes or neural stem cells (Figure 5A).

We next examined whether p11 expression in hippocampal neuronal subpopulations is altered in response to antidepressant

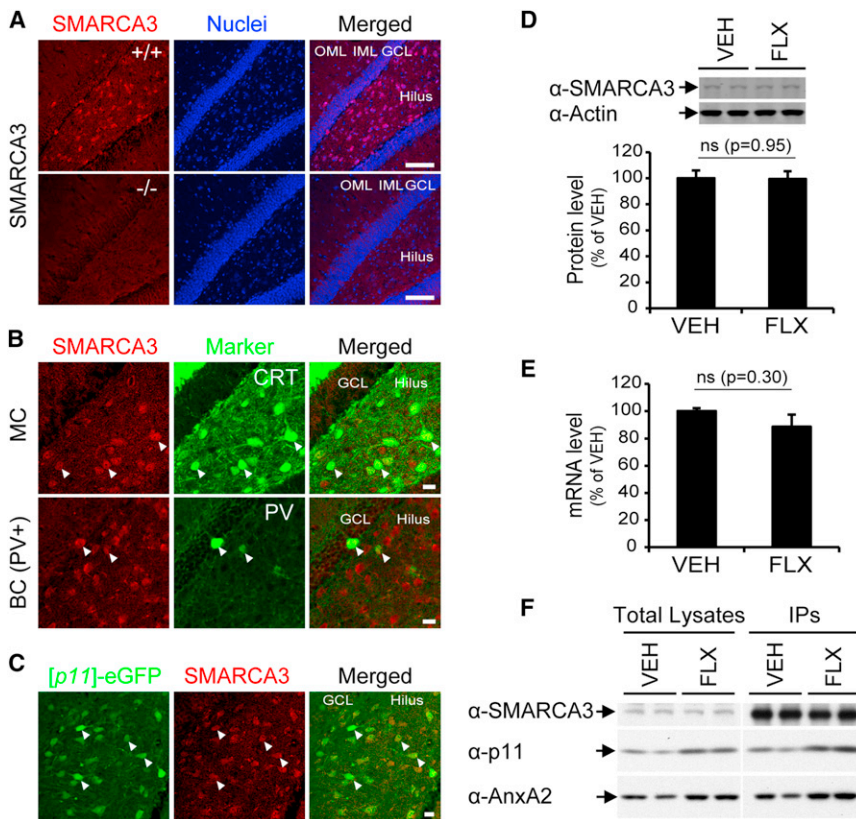


Figure 6. SMARCA3 Expression in Mossy Cells and Basket Cells in the Dentate Gyrus

(A) Dentate gyrus slices from WT (top) or *SMARCA3* KO mice (bottom) stained with anti-*SMARCA3* antibody (red) and nuclear dye DraQ5 (blue). Scale bars, 100 μ m.

(B) Neuronal cell types expressing *SMARCA3* in the dentate gyrus. Scale bars, 20 μ m. Representative cells doubly labeled are indicated by arrowheads.

(C) Coexpression of [p11]-EGFP and *SMARCA3*. BAC-[p11]-EGFP mice were stained with anti-EGFP and anti-*SMARCA3* antibodies. Representative cells doubly labeled are indicated by arrowheads. Scale bar, 20 μ m.

(D and E) Level of *SMARCA3* is not altered by FLX administration for 2 weeks. Hippocampal lysates were immunoblotted for *SMARCA3* and β -actin (D). mRNA level of *SMARCA3* in the hippocampus was measured using qPCR (E). Data represent mean \pm SEM ($n = 6$ –7 mice per group). ns, nonsignificant.

(F) Formation of p11/AnxA2/*SMARCA3* complex is increased after treatment with FLX for 2 weeks. *SMARCA3* was immunoprecipitated from hippocampal lysates. Total lysates and immunoprecipitates (IPs) were immunoblotted for *SMARCA3*, p11, and AnxA2.

See also Figure S5.

administration. We took advantage of the distinct laminar segregation of the two types of p11-expressing neurons. The mossy cells assessed by CRT expression locate their soma and dendrites within the deep hilus and project their axonal arbor to the inner molecular layer (IML), whereas a subpopulation of basket cells visualized by PV staining locates its somas in the hilar border and projects its axons to the granule cells within the granular cell layer (GCL) (Figure 5B). Because p11 is mainly enriched in mossy cells and basket cells, the [p11]-EGFP signal in the hilus and IML represents p11 promoter activity in mossy cells, and the signal of EGFP in GCL does for basket cell activity. BAC-[p11]-EGFP mice were treated with FLX for 2 weeks, and [p11]-EGFP signal was examined in the areas of hilus, IML, and GCL (Figures 5C–5E). Because a high density of serotonergic innervation prevails in the caudal part of the hippocampal formation, whereas the rostral part receives only a moderate-to-weak serotonergic innervation (Bjarkam et al., 2003; Gage and Thompson, 1980), the caudal part (bregma -2.5 to -4.0) of the dentate gyrus was used for the analysis. FLX treatment increased [p11]-EGFP in the dentate gyrus (Figures 5C and 5D). Quantitative analysis revealed that FLX increased [p11]-EGFP intensity in hilus and IML as well as in GCL, suggesting p11 induction in mossy cells and basket cells (Figure 5E). p11 is also induced in the rostral part of the hippocampus but with less potency (Figure S4B). AnxA2, together with p11, is induced by FLX and requires p11 for its protein stability (Figures 1D and 1E). Conversely, p11 protein requires AnxA2 for its protein stability (data not

shown). Thus, AnxA2 is also likely to be induced in the same neurons.

We examined the expression of *SMARCA3* in the dentate gyrus by immunohistochemistry. The specificity of the immunostaining was tested using *SMARCA3* KO mice. *SMARCA3* KO mice were generated by targeting exons 11–13 of the *SMARCA3* gene (Figure S5A). Immunoblotting (Figures S5B and S5C) and immunohistochemistry (Figure 6A) confirmed the absence of *SMARCA3*. *SMARCA3* is expressed primarily in the hilar area of the dentate gyrus (Figure 6A), where it is enriched in mossy cells and parvalbumin-positive basket cells (Figure 6B), and is expressed in [p11]-EGFP-positive cells (Figure 6C).

In contrast to p11 and AnxA2 (Figures 1D and 1E), the levels of *SMARCA3* protein (Figure 6D) and mRNA (Figure 6E) were not altered after treatment with FLX. Analysis of hippocampal lysates, following immunoprecipitation of *SMARCA3*, revealed that chronic FLX administration increased the ternary complex of p11/AnxA2/*SMARCA3* by about 2.3-fold (Figure 6F). Thus, p11 and AnxA2 induction facilitates the assembly of the p11/AnxA2/*SMARCA3* complex. Taken together, these results identify the mossy cells and the basket cells in the dentate gyrus as primary neuronal types for SSRI/p11/*SMARCA3* signaling.

SMARCA3 Is Required for Neurogenic and Behavioral Response to Chronic SSRI Administration

p11 KO results in the loss of enhanced hippocampal neurogenesis and behavioral change in response to chronic antidepressant treatment (Egeland et al., 2010), suggesting a crucial role

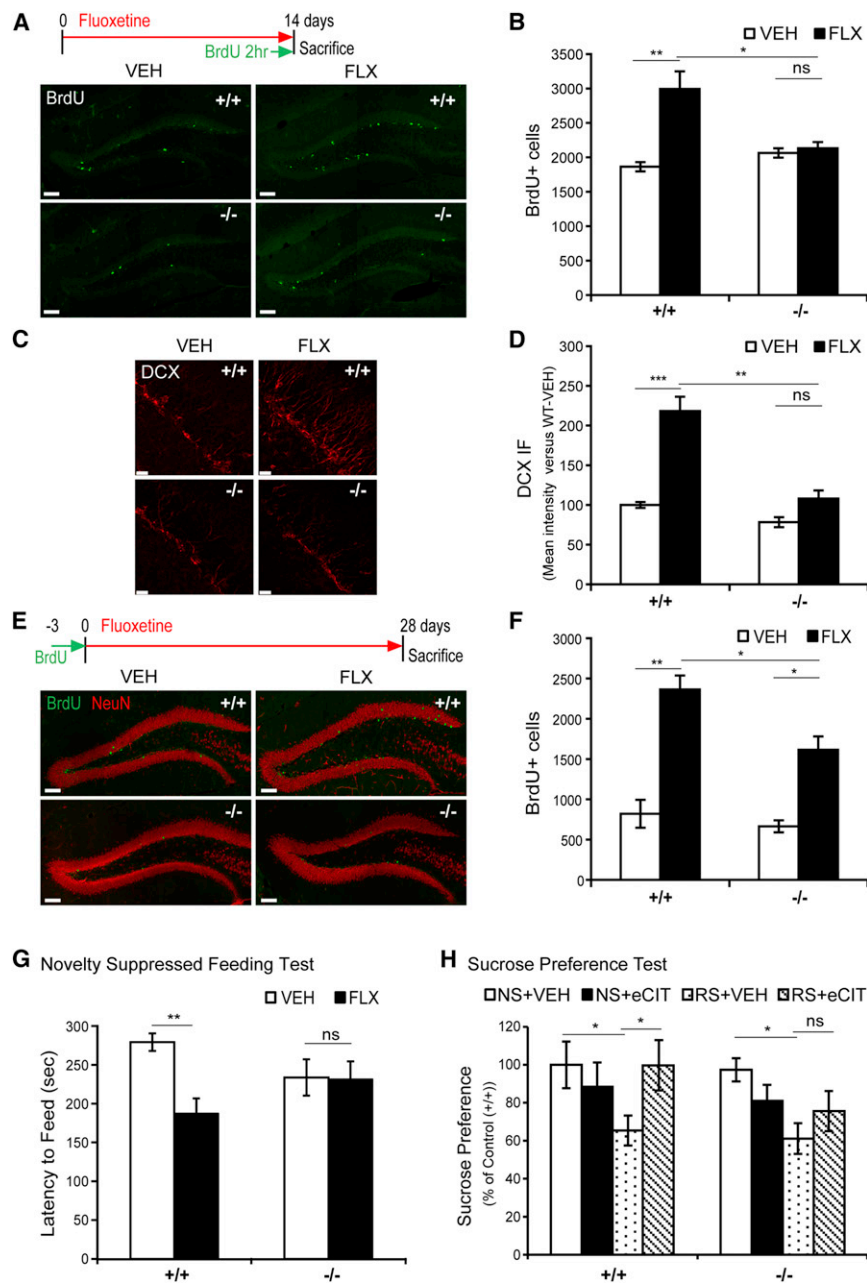


Figure 7. SMARCA3 Is Required for SSRI-Induced Neurogenesis and Behavioral Changes

(A and B) FLX-induced cell proliferation in WT and *SMARCA3* KO mice. WT (+/+) and *SMARCA3* KO (-/-) mice were administered VEH or FLX for 14 days and labeled with BrdU for the last 2 hr prior to perfusion. (A) Immunostaining with anti-BrdU. Scale bars, 100 μ m. (B) Quantitation of BrdU-positive cells in the subgranular zone ($n = 6-8$ mice per group).

(C and D) FLX-induced increase of DCX-positive cells in WT and *SMARCA3* KO mice. (C) Immunostaining with anti-DCX. Scale bars, 20 μ m. (D) Quantitation of DCX-positive cells in the subgranular and granular zone ($n = 6-8$ per group). (E and F) Survival of newborn cells in WT and *SMARCA3* KO mice treated with VEH or FLX. BrdU was injected for three consecutive days prior to FLX administration for 28 days. (E) Immunostaining with anti-BrdU and anti-NeuN. Scale bars, 100 μ m. (F) Quantitation of BrdU-positive cells.

(G and H) Behavior was assayed using (G) the NSF paradigm after chronic administration of VEH or FLX (4 weeks, $n = 14-16$ per group), or (H) the SPT in NS or RS mice after chronic administration of VEH or eCIT (4 weeks, $n = 8-11$ per group).

All data represent mean \pm SEM. * $p < 0.05$, ** $p < 0.01$, and *** $p < 0.001$, two-way ANOVA followed by the post hoc Bonferroni test. ns, nonsignificant. See also Figure S6 and Table S3.

treated with FLX (160.6% \pm 13.7% of VEH group; $p < 0.01$), but not in *SMARCA3* KO mice (Figures 7A and 7B). We also carried out an alternative assay measuring an endogenous mitotic marker Ki-67. Ki-67-positive cells were significantly increased in response to FLX in WT mice (143.8% \pm 8.6%; $p < 0.01$), but not in *SMARCA3* KO mice (Figures S6A and S6B), confirming the results of the BrdU assay.

We next analyzed the expression level of doublecortin (DCX), a marker for immature neurons, which represents a snapshot of newborn cells undergoing neuronal maturation and differentiation

for p11 and its downstream signaling pathways in those antidepressant actions. We examined here whether *SMARCA3*, as a downstream signaling molecule of p11, might mediate chronic antidepressant-induced hippocampal neurogenesis and behaviors.

Adult neurogenesis is controlled by multistep processes including the proliferation of neural progenitors, differentiation, and maturation into functional granule neurons (Ming and Song, 2011). We examined proliferation using *in vivo* BrdU labeling of the neural progenitors in the S phase in WT and *SMARCA3* KO mice. A significant increase was observed in the number of BrdU-labeled neural progenitors in WT mice

(Couillard-Despres et al., 2005). DCX immunofluorescence signal was increased by chronic FLX administration in WT mice (218.4% \pm 18.0%; $p < 0.001$), but not in *SMARCA3* KO mice (Figures 7C and 7D). Chronic FLX administration promotes the newborn cells to survive at postmitotic stages and also to become mature neurons (Wang et al., 2008). Chronic FLX administration greatly increased the survival of the BrdU-labeled newborn cells in WT mice (288.2% \pm 21.1%; $p < 0.01$), but the effect of FLX was attenuated in *SMARCA3* KO mice (196.0% \pm 20.3%; $p < 0.05$) (Figures 7E and 7F). Taken together, these results indicate that *SMARCA3* contributes to multiple stages of antidepressant-stimulated neurogenesis, and this phenotype

of *SMARCA3* KO mice is reminiscent of that observed in *p11* KO mice (Egeland et al., 2010).

Next, we investigated the functional significance of the p11/AnxA2/*SMARCA3* complex for SSRI-induced behavioral changes. WT and *SMARCA3* KO mice did not display a baseline difference in locomotor activity (open field test, Figure S6C), depressive behaviors (tail suspension test [TST] and sucrose preference test [SPT], Figures S6D and S6E), or anxiety behaviors (light/dark and elevated plus maze tests, Figures S6F and S6G). Novelty-suppressed feeding (NSF) is believed to represent depression-like and anxiety behavior, and this test is commonly used to measure the chronic effect of antidepressants (David et al., 2009; Surget et al., 2011). *p11* KO mice are refractory to behavioral change in response to chronic FLX administration in the NSF test (Egeland et al., 2010; Schmidt et al., 2012). In the same model, we analyzed the behavior of *SMARCA3* KO mice. Chronic treatment with FLX shortened latency to feed compared to VEH treatment in WT mice (VEH versus FLX, 279 ± 13 versus 187 ± 20 ; $p < 0.01$), but not in *SMARCA3* KO mice (Figure 7G), as with *p11* KO mice (Egeland et al., 2010). Neither FLX nor *SMARCA3* KO caused any significant effect on home cage feeding (Figure S6H) or body weight (data not shown).

Anhedonia is a core symptom of human depression (Berton and Nestler, 2006), and a chronic stress-induced decrease in sucrose preference in rodents is regarded as a sign of a hedonic deficit (Katz, 1982), which can be treated with chronic SSRI. We examined the effect of chronic administration of escitalopram (eCIT, another SSRI) on the behaviors of nonstressed (NS) or restraint-stressed (RS) mice in the SPT. Daily restraint for 14 days induced a reduction of sucrose consumption in both WT (NS plus VEH versus RS plus VEH, $100\% \pm 12\%$ versus $68\% \pm 8\%$, respectively) and *SMARCA3* KO mice (NS plus VEH versus RS plus VEH, $97\% \pm 6\%$ versus $61\% \pm 8\%$, respectively). Poststress treatment with eCIT recovered sucrose consumption to the normal level in WT mice (RS plus VEH versus RS plus eCIT, $68\% \pm 8\%$ versus $99\% \pm 13\%$, respectively), but not in *SMARCA3* KO mice (Figure 7H). No differences were observed between WT and *SMARCA3* KO mice as well as among the experimental groups used for the SPT with regard to their locomotor activities (Figure S6I). Notably, the behavioral despair in the TST is known to be treated by acute SSRI, whereas the therapeutic effect of SSRI in the NSF and SPT requires chronic treatment. *SMARCA3* KO did not alter the effect of acute administration of eCIT in the TST (Figure S6J). Taken together, our results suggest a crucial role for *SMARCA3* in p11-dependent neurogenic and behavioral response to chronic antidepressant administration.

DISCUSSION

Molecular Interaction of p11/AnxA2 with *SMARCA3*

p11 and AnxA2 cooperate to create a unique binding pocket, but the optimal binding condition is not achieved without conformational changes associated with target binding. Upon interaction with the *SMARCA3* peptide, both Asp60 in p11 and Ser12 in AnxA2 flip inward toward the peptide-binding groove, forming additional intermolecular hydrogen bonds (Figures 3D–3F). Similar intermolecular contacts were also observed in

the AHNAK1 complex (Figures S2D–S2F). These findings support an induced-fit model for the assembly of the p11/AnxA2/*SMARCA3* complex. Among the key residues found in the binding pocket, the role of Ser12 (AnxA2) is of particular interest because this residue is regulated by phosphorylation (Jost and Gerke, 1996), which may interfere with high-affinity binding of ternary targets.

The current study identifies a binding motif, which is represented as ϕ -P-#-F-X-F, and can be used for in silico analysis to identify binding targets of p11/AnxA2. Our binding motif is different from the p11-binding sequences previously reported for TRPV5/6 (VATTV) (van de Graaf et al., 2003) and TASK1 (RRSSV) (Girard et al., 2002). It is possible that the p11/AnxA2 heterotetramer has additional binding pocket(s) on the surface.

Regulation of *SMARCA3* Function by Interaction with the p11/AnxA2 Complex

Most chromatin remodelers, including four well-characterized subfamily members (SWI/SNF, INO80/SWR1, ISWI, and CHD), form a large multisubunit complex with a core ATPase motor subunit and unique accessory/regulatory subunits (Hargreaves and Crabtree, 2011). The core subunit displays DNA- and nucleosome-dependent ATPase activity, and the accessory/regulatory subunits are essential for the function of the core ATPase subunit, by facilitating the interaction with the transcriptional regulatory factors, mediating the indirect binding to DNA and/or modified histones, and targeting the complex to subnuclear locations (Mohrmann and Verrijzer, 2005). *SMARCA3*, a relatively uncharacterized member of the SWI/SNF protein family, is composed of multiple functional domains, including a DNA-binding domain, a SWI2/SNF2 ATPase domain, a RING-type zinc finger domain for the binding to RFBP, a Type IV P-type ATPase, and a C-terminal domain for the binding of transcription factors such as Sp1, Sp3, Egr1, and cRel (Debaue et al., 2008) (Figure 2D). Although p11 and AnxA2 stabilize each other as structural components of a protein complex (Figure 1), the levels of p11 and AnxA2 are not altered in *SMARCA3* KO mice (Figures S5B and S5C), and the level of *SMARCA3* is not altered in *p11* KO mice (data not shown). Thus, p11 and AnxA2 act as regulatory proteins but are not likely structural core components of *SMARCA3*. Notably, the DNA-binding domain at the N-terminal side of the ATPase domain mediates the sequence-dependent binding of *SMARCA3* to the target DNA (Debaue et al., 2008). p11/AnxA2 facilitates the DNA-binding affinity of *SMARCA3* (Figures 4A and 4B). Most chromatin-remodeling complexes, including *SMARCA3*, display DNA- and/or nucleosome-dependent ATPase activity (Hargreaves and Crabtree, 2011). Therefore, it is conceivable that the enhanced DNA binding of *SMARCA3*, upon the interaction with p11/AnxA2, may lead to the activation of *SMARCA3* to initiate ATP-dependent chromatin remodeling of the target genes. Thus, p11/AnxA2 binding to *SMARCA3* would open the chromatin structure and recruit specific transcription factors bound to the C-terminal domain of *SMARCA3* to the specific locus of the genomic DNA.

Critical nuclear events such as gene expression, replication, and repair processing occur at a distinct subnuclear region, the nuclear matrix, which is composed of nuclear lamins, nuclear actin/actin-related proteins, and phospholipids

(Barlow et al., 2010; Zaidi et al., 2007). Indeed, key gene regulatory machineries such as transcription factors, chromatin-remodeling complexes, RNA polymerase II, and processing factor SC35 are associated with nuclear matrix structures (Zaidi et al., 2007). p11/AnxA2 mediates the subnuclear targeting of SMARCA3 (Figures 4C and 4D). The subnuclear targeting of SMARCA3 is likely controlled by intrinsic phospholipid- and actin-binding properties of AnxA2 (Gerke et al., 2005). Our crystal structure of p11/full-length AnxA2/SMARCA3 peptide visualized the spatial organization of each component in the ternary complex, in which the p11 dimer is ideally positioned in the core of the complex to link SMARCA3 to AnxA2 (Figure 3G). Thus, our current model is reminiscent of the role of p11/AnxA2 in mediating the membrane translocation of AHNAK1 (Benaud et al., 2004). Both SMARCA3 and AHNAK1 use the interaction with p11/AnxA2 to localize properly to the distinct subcellular sites where they become functionally active.

p11/AnxA2/SMARCA3 Complex in Antidepressant Action

p11/AnxA2/SMARCA3 complex-mediated hippocampal neurogenesis may contribute to the behavioral response to SSRIs. However, the involvement of hippocampal neurogenesis in depression and antidepressant-induced behavioral change is still controversial (Hanson et al., 2011). Such neurogenesis has been associated with mood, stress responses, and antidepressant effects in some studies (Santarelli et al., 2003; Snyder et al., 2011; Surget et al., 2011), but not in others (Bessa et al., 2009).

p11 and SMARCA3 are enriched in mossy cells and basket cells but not detectable in neural progenitor cells. Thus, the regulation of SSRI-induced neurogenesis by the p11/AnxA2/SMARCA3 signaling pathway is non-cell autonomous. In fact, GABAergic interneurons play an important role in the differentiation, development, and integration of newborn neurons (Ge et al., 2006; Tozuka et al., 2005). Specifically, interneuronal GABA release is thought to act directly on neural progenitor cells and, due to an age-specific increase in intracellular chloride levels in these young cells, causes an atypical depolarization that subsequently affects neurogenic processes (Tozuka et al., 2005). The synaptic regulation of granule cells by basket and mossy cells may contribute to the neurogenic and behavioral responses to SSRIs. It has been suggested that, upon activation by local inputs from the granule cells in the dentate gyrus, glutamatergic mossy cells primarily provide excitatory feedback to the granule cells through their axonal projections to the IML and also provide excitatory drive to local GABAergic HIPPs in the hilus (Henze and Buzsáki, 2007; Scharfman, 1995). The basket cells primarily provide feedforward inhibition to the granule cells in response to excitatory inputs from the entorhinal cortex and feedback inhibition to the granule cells in response to excitatory inputs from the granule cells (Houser, 2007). Thus, despite their relatively low abundance ($\sim 3 \times 10^4$ mossy cells and 0.5×10^4 basket cells versus 1×10^6 granule cells in rat), the mossy cells and basket cells regulate the flow of extrinsic input to the dentate gyrus through modulation of the activity of the granule cells and/or the HIPPs, and such regulation is important to generate the distinct oscillation patterns of neuronal excitation in the dentate gyrus (Amaral et al., 2007; Henze and Buzsáki, 2007).

In this study, we have identified and characterized a nuclear protein complex mediating chronic actions of SSRIs. Many interesting questions have been raised as a result of this study: What are the roles of p11 and SMARCA3 in the excitability and synaptic transmission of basket cells and mossy cells? Which genes are regulated by the p11/AnxA2/SMARCA3 complex in basket cells and mossy cells? Which of these genes contribute to the neurogenic and behavioral responses to antidepressants?

Current and future studies of the p11/AnxA2/SMARCA3 pathway should contribute not only to our understanding of SSRI actions but also provide molecular and cellular targets for the development of advanced therapeutics for mood and anxiety disorders.

EXPERIMENTAL PROCEDURES

Generation of Transgenic Mice

All procedures involving animals were approved by the Rockefeller University Institutional Animal Care and Use Committee and were in accordance with the National Institutes of Health guidelines. The constitutive *SMARCA3* KO mice were generated in Taconic-Artemis (Germany) and maintained at The Rockefeller University. The BAC-*p11*-EGFP transgenic line (GENSAT; Clone No. HC85) was provided by GENSAT (Gong et al., 2002). The mouse breeding and drug treatment methods are in the [Extended Experimental Procedures](#).

Crystallization and Structure Determination of p11/AnxA2/SMARCA3 and p11/AnxA2/AHNAK1 Complexes

Details of protein preparations, protein expression, purification, crystallization conditions, data collection, and refinement are included in [Extended Experimental Procedures](#).

Preparation of Nuclear Matrix Fraction

Cells were incubated with cell-permeable crosslinker, DSP (1 mM), and extracted with CSK buffer containing 0.5% NP40. After chromatin digestion with DNase I and then elution with 0.25 M $(\text{NH}_4)_2\text{SO}_4$, the nuclear matrix fraction was scraped for the biochemical assay or fixed with 2% paraformaldehyde for immunocytochemistry (detailed description is in [Extended Experimental Procedures](#)).

Histological Methods

Immunostaining was carried out using the standard free-floating method. Detailed description of antibody preparation, antigen retrieval, image acquisition, and quantification is in [Extended Experimental Procedures](#).

Behavioral Analysis

Mood and anxiety-related behaviors (NSF, SPT, TST, light-dark box test, and elevated plus maze) and locomotor activity (open field test) were tested as described in [Extended Experimental Procedures](#).

Data Analysis and Statistics

All data are presented as mean \pm SEM. Two group comparisons were done by two-tailed, unpaired Student's *t* test. Multiple group comparisons were assessed using a one-way or two-way ANOVA, followed by the post hoc Newman-Keuls test or Bonferroni test, respectively, when significant main effects or interactions were detected. Statistical significance was set at $p < 0.05$ level. Summary of statistical analysis for animal experiments is included as [Table S3](#).

ACCESSION NUMBERS

Coordinates and structure factors for p11-AnxA2 peptide cassette in complex with AHNAK1 peptide (PDB 4HRG) and SMARCA3 peptide (PDB 4HRH) and full-length p11/AnxA2 heterotetramer in complex with SMARCA3 peptide (PDB 4HRE) have been deposited in the RCSB Protein Data Bank.

SUPPLEMENTAL INFORMATION

Supplemental Information includes Extended Experimental Procedures, six figures, and three tables and can be found with this article online at <http://dx.doi.org/10.1016/j.cell.2013.01.014>.

ACKNOWLEDGMENTS

This work was supported by DOD/USAMRAA Grant W81XWH-09-1-0392 to Y.K.; DOD/USAMRAA Grant W81XWH-09-1-0402 to P. Greengard; the JPB Foundation to P. Greengard; the Fisher Center Foundation to P. Greengard; NIH grants (MH090963, DA10044, and AG09464) to Y.K. and P. Greengard; and the Maloris Foundation and the Abby Rockefeller Mauze Trust to D.J.P. We thank the staff at beamline 24ID-C of the Advanced Photon Source at the Argonne National Laboratory and beamline X29 of the National Synchrotron Light Source at the Brookhaven National Laboratory for assistance with data collection. We thank Daesoo Kim, Eric Schmidt, Jennifer Wagner-Schmidt, and Yotam Sagi for their helpful advice and discussion, and Elisabeth Griggs for technical assistance. We would like to thank Ji-Eun Kim for the mass spectrometry analysis. Finally, we would like to acknowledge Rada Norinsky and the Rockefeller University Transgenics Services Laboratory for their excellent IVF services; and Henry Zebroski III and Nagarajan Chandramouli from The Rockefeller University Proteomics Resource Center.

Received: May 16, 2012

Revised: September 14, 2012

Accepted: January 8, 2013

Published: February 14, 2013

REFERENCES

- Amaral, D.G., Scharfman, H.E., and Lavenex, P. (2007). The dentate gyrus: fundamental neuroanatomical organization (dentate gyrus for dummies). *Prog. Brain Res.* **163**, 3–22.
- Barlow, C.A., Laishram, R.S., and Anderson, R.A. (2010). Nuclear phosphoinositides: a signaling enigma wrapped in a compartmental conundrum. *Trends Cell Biol.* **20**, 25–35.
- Benaud, C., Gentil, B.J., Assard, N., Court, M., Garin, J., Delphin, C., and Baudier, J. (2004). AHNAK interaction with the annexin 2/S100A10 complex regulates cell membrane cytoarchitecture. *J. Cell Biol.* **164**, 133–144.
- Berton, O., and Nestler, E.J. (2006). New approaches to antidepressant drug discovery: beyond monoamines. *Nat. Rev. Neurosci.* **7**, 137–151.
- Bessa, J.M., Ferreira, D., Melo, I., Marques, F., Cerqueira, J.J., Palha, J.A., Almeida, O.F., and Sousa, N. (2009). The mood-improving actions of antidepressants do not depend on neurogenesis but are associated with neuronal remodeling. *Mol. Psychiatry* **14**, 764–773.
- Bjarkam, C.R., Sørensen, J.C., and Geneser, F.A. (2003). Distribution and morphology of serotonin-immunoreactive axons in the hippocampal region of the New Zealand white rabbit. I. Area dentata and hippocampus. *Hippocampus* **13**, 21–37.
- Couillard-Despres, S., Winner, B., Schauback, S., Aigner, R., Vroemen, M., Weidner, N., Bogdahn, U., Winkler, J., Kuhn, H.G., and Aigner, L. (2005). Doublecortin expression levels in adult brain reflect neurogenesis. *Eur. J. Neurosci.* **21**, 1–14.
- Das, S., Shetty, P., Valapala, M., Dasgupta, S., Gryczynski, Z., and Vishwanatha, J.K. (2010). Signal transducer and activator of transcription 6 (STAT6) is a novel interactor of annexin A2 in prostate cancer cells. *Biochemistry* **49**, 2216–2226.
- David, D.J., Samuels, B.A., Rainer, Q., Wang, J.W., Marsteller, D., Mendez, I., Drew, M., Craig, D.A., Guiard, B.P., Guilloux, J.P., et al. (2009). Neurogenesis-dependent and -independent effects of fluoxetine in an animal model of anxiety/depression. *Neuron* **62**, 479–493.
- Debaue, G., Capouillez, A., Belayew, A., and Saussez, S. (2008). The helicase-like transcription factor and its implication in cancer progression. *Cell. Mol. Life Sci.* **65**, 591–604.
- Ding, H., Descheemaeker, K., Marynen, P., Nelles, L., Carvalho, T., Carmo-Fonseca, M., Collen, D., and Belayew, A. (1996). Characterization of a helicase-like transcription factor involved in the expression of the human plasminogen activator inhibitor-1 gene. *DNA Cell Biol.* **15**, 429–442.
- Egeland, M., Warner-Schmidt, J., Greengard, P., and Svenningsson, P. (2010). Neurogenic effects of fluoxetine are attenuated in p11 (S100A10) knockout mice. *Biol. Psychiatry* **67**, 1048–1056.
- Gage, F.H., and Thompson, R.G. (1980). Differential distribution of norepinephrine and serotonin along the dorsal-ventral axis of the hippocampal formation. *Brain Res. Bull.* **5**, 771–773.
- Ge, S., Goh, E.L., Sailor, K.A., Kitabatake, Y., Ming, G.L., and Song, H. (2006). GABA regulates synaptic integration of newly generated neurons in the adult brain. *Nature* **439**, 589–593.
- Gerke, V., Creutz, C.E., and Moss, S.E. (2005). Annexins: linking Ca²⁺ signaling to membrane dynamics. *Nat. Rev. Mol. Cell Biol.* **6**, 449–461.
- Girard, C., Tinel, N., Terrenoire, C., Romey, G., Lazdunski, M., and Borsotto, M. (2002). p11, an annexin II subunit, an auxiliary protein associated with the background K⁺ channel, TASK-1. *EMBO J.* **21**, 4439–4448.
- Gong, S., Yang, X.W., Li, C., and Heintz, N. (2002). Highly efficient modification of bacterial artificial chromosomes (BACs) using novel shuttle vectors containing the R6Kgamma origin of replication. *Genome Res.* **12**, 1992–1998.
- Hanson, N.D., Owens, M.J., and Nemeroff, C.B. (2011). Depression, antidepressants, and neurogenesis: a critical reappraisal. *Neuropsychopharmacology* **36**, 2589–2602.
- Hargreaves, D.C., and Crabtree, G.R. (2011). ATP-dependent chromatin remodeling: genetics, genomics and mechanisms. *Cell Res.* **21**, 396–420.
- Heintz, N. (2001). BAC to the future: the use of bac transgenic mice for neuroscience research. *Nat. Rev. Neurosci.* **2**, 861–870.
- Henze, D.A., and Buzsáki, G. (2007). Hilar mossy cells: functional identification and activity in vivo. *Prog. Brain Res.* **163**, 199–216.
- Houser, C.R. (2007). Interneurons of the dentate gyrus: an overview of cell types, terminal fields and neurochemical identity. *Prog. Brain Res.* **163**, 217–232.
- Jost, M., and Gerke, V. (1996). Mapping of a regulatory important site for protein kinase C phosphorylation in the N-terminal domain of annexin II. *Biochim. Biophys. Acta* **1313**, 283–289.
- Katz, R.J. (1982). Animal model of depression: pharmacological sensitivity of a hedonic deficit. *Pharmacol. Biochem. Behav.* **16**, 965–968.
- Kube, E., Becker, T., Weber, K., and Gerke, V. (1992). Protein-protein interaction studied by site-directed mutagenesis. Characterization of the annexin II-binding site on p11, a member of the S100 protein family. *J. Biol. Chem.* **267**, 14175–14182.
- Liu, J., and Vishwanatha, J.K. (2007). Regulation of nucleo-cytoplasmic shuttling of human annexin A2: a proposed mechanism. *Mol. Cell. Biochem.* **303**, 211–220.
- Ming, G.L., and Song, H. (2011). Adult neurogenesis in the mammalian brain: significant answers and significant questions. *Neuron* **70**, 687–702.
- Mohrmann, L., and Verrijzer, C.P. (2005). Composition and functional specificity of SWI2/SNF2 class chromatin remodeling complexes. *Biochim. Biophys. Acta* **1681**, 59–73.
- Rando, O.J., Zhao, K., Janmey, P., and Crabtree, G.R. (2002). Phosphatidylinositol-dependent actin filament binding by the SWI/SNF-like BAF chromatin remodeling complex. *Proc. Natl. Acad. Sci. USA* **99**, 2824–2829.
- Rescher, U., and Gerke, V. (2008). S100A10/p11: family, friends and functions. *Pflugers Arch.* **455**, 575–582.
- Réty, S., Sopkova, J., Renouard, M., Osterloh, D., Gerke, V., Tabaries, S., Russo-Marie, F., and Lewit-Bentley, A. (1999). The crystal structure of a complex of p11 with the annexin II N-terminal peptide. *Nat. Struct. Biol.* **6**, 89–95.
- Rezvanpour, A., Phillips, J.M., and Shaw, G.S. (2009). Design of high-affinity S100-target hybrid proteins. *Protein Sci.* **18**, 2528–2536.

- Santarelli, L., Saxe, M., Gross, C., Surget, A., Battaglia, F., Dulawa, S., Weisstaub, N., Lee, J., Duman, R., Arancio, O., et al. (2003). Requirement of hippocampal neurogenesis for the behavioral effects of antidepressants. *Science* 301, 805–809.
- Scharfman, H.E. (1995). Electrophysiological evidence that dentate hilar mossy cells are excitatory and innervate both granule cells and interneurons. *J. Neurophysiol.* 74, 179–194.
- Schmidt, E.F., Warner-Schmidt, J.L., Otopalik, B.G., Pickett, S.B., Greengard, P., and Heintz, N. (2012). Identification of the cortical neurons that mediate antidepressant responses. *Cell* 149, 1152–1163.
- Snyder, J.S., Soumier, A., Brewer, M., Pickel, J., and Cameron, H.A. (2011). Adult hippocampal neurogenesis buffers stress responses and depressive behaviour. *Nature* 476, 458–461.
- Surget, A., Tanti, A., Leonardo, E.D., Laugeray, A., Rainer, Q., Touma, C., Palme, R., Griebel, G., Ibarguen-Vargas, Y., Hen, R., and Belzung, C. (2011). Antidepressants recruit new neurons to improve stress response regulation. *Mol. Psychiatry* 16, 1177–1188.
- Svenningsson, P., Chergui, K., Rachleff, I., Flajolet, M., Zhang, X., El Yacoubi, M., Vaugeois, J.M., Nomikos, G.G., and Greengard, P. (2006). Alterations in 5-HT_{1B} receptor function by p11 in depression-like states. *Science* 311, 77–80.
- Tozuka, Y., Fukuda, S., Namba, T., Seki, T., and Hisatsune, T. (2005). GABAergic excitation promotes neuronal differentiation in adult hippocampal progenitor cells. *Neuron* 47, 803–815.
- van de Graaf, S.F., Hoenderop, J.G., Gkika, D., Lamers, D., Prenen, J., Rescher, U., Gerke, V., Staub, O., Nilius, B., and Bindels, R.J. (2003). Functional expression of the epithelial Ca²⁺ channels (TRPV5 and TRPV6) requires association of the S100A10-annexin 2 complex. *EMBO J.* 22, 1478–1487.
- Wang, J.W., David, D.J., Monckton, J.E., Battaglia, F., and Hen, R. (2008). Chronic fluoxetine stimulates maturation and synaptic plasticity of adult-born hippocampal granule cells. *J. Neurosci.* 28, 1374–1384.
- Warner-Schmidt, J.L., Chen, E.Y., Zhang, X., Marshall, J.J., Morozov, A., Svenningsson, P., and Greengard, P. (2010). A role for p11 in the antidepressant action of brain-derived neurotrophic factor. *Biol. Psychiatry* 68, 528–535.
- Zaidi, S.K., Young, D.W., Javed, A., Pratap, J., Montecino, M., van Wijnen, A., Lian, J.B., Stein, J.L., and Stein, G.S. (2007). Nuclear microenvironments in biological control and cancer. *Nat. Rev. Cancer* 7, 454–463.
- Zhao, K., Wang, W., Rando, O.J., Xue, Y., Swiderek, K., Kuo, A., and Crabtree, G.R. (1998). Rapid and phosphoinositol-dependent binding of the SWI/SNF-like BAF complex to chromatin after T lymphocyte receptor signaling. *Cell* 95, 625–636.